Classical Trajectory Study of the Cis−Trans Isomerization and F−O Dissociation of FONO

Angeles Peña-Gallego, Emilio Martínez-Núñez, and Saulo A. Vázquez*

Departamento de Química Física, Universidad de Santiago de Compostela, Santiago de Compostela E-15706, Spain

Received: June 8, 1998; In Final Form: August 5, 1998

Classical trajectory calculations were carried out to investigate whether nonstatistical behavior is exhibited in two unimolecular processes of nitrosyl hypofluorite: (I) cis−trans isomerization and (II) F−O bond dissociation to produce F and ONO. For this purpose, an analytical potential function that describes these two processes was developed based on ab initio and experimental data reported in the literature. Total and individual rate constants were evaluated under two different types of initial sampling conditions: microcanonical (statistical) distribution of vibrational energy and selective excitation of vibrational modes. Under statistical initial conditions, the rates of isomerization are calculated to be substantially larger than the rates of F−O dissociation, although the branching ratios decrease as energy increases. In addition, the isomerization and dissociation reactions are faster when they occur from the trans isomer. Dissociation was found to be slightly faster than isomerization when energy was selectively deposited in certain vibrational modes of *trans*-FONO. Our results predict that both intrinsic and apparent non-RRKM behavior are present in the dynamics of the processes studied.

Introduction

The Rice−Ramsperger−Kassel−Marcus (RRKM) formulation[1] of unimolecular reactions, one of the most successful theories in chemical kinetics, assumes that the vibrational energy is rapidly randomized on the time scale of reaction throughout all vibrational degrees of freedom, so that molecules with a particular energy have a distribution $P(\tau)$ of lifetimes τ given by[2]

$$P(\tau) = k \exp(-k\tau) \tag{1}$$

where k is the RRKM rate constant. A unimolecular process that evolves in this way is classified as intrinsically RRKM.[3,4] Such is the case of most unimolecular processes in which the barrier to reaction is high, so that the excitation energy can be distributed among all the modes of the molecule before sufficient energy is transferred to the reaction coordinate modes leading to reaction. However, in reactions with relatively low energy barriers, the rate of intramolecular vibrational energy redistribution (IVR) may limit the reaction rate, and as a result, non-RRKM behavior is exhibited.

Bunker and Hase[3,4] characterized two types of non-RRKM behavior: intrinsic and apparent. The former is shown when the molecule possesses weak coupling between certain vibrational states, in other words, when there is a bottleneck (or bottlenecks) in the flow of energy between vibrational states. Apparent non-RRKM behavior can arise when the molecular states are excited nonrandomly and IVR is not significantly rapid as compared with the rate of reaction.

Over the last years, the development of new methods of energy and state preparation as well as the improvement of theoretical techniques have entailed increasing attention to the study of mode-specific chemistry. Cis−trans isomerizations over low barriers are among the unimolecular processes that may be potentially interesting candidates to explore nonstatistical behavior. In particular, Shirk et al.[5,6] studied the cis−trans interconvertion of HONO in solid nitrogen and argon by selective vibrational excitation, and they observed that mode specific effects are present in the dynamics of isomerization. Thompson et al.[7−9] performed classical trajectory calculations to explore the isomerization of HONO at much higher energies than used in the above experimental work. They found that the rates of cis−trans conversions are strongly dependent on the site of initial excitation. Similar calculations on the isomerization of CH_3ONO[10,11] indicate that apparent non-RRKM behavior is exhibited upon excitation of various vibrational modes.

We thought it interesting to explore the possibility of mode-specific effects in the related molecules XONO (X = F, Cl, Br), which are of some interest as minor constituents in stratospheric chemistry.[12] All of these molecules are characterized by relatively low barriers to cis−trans isomerization and low X−O bond dissociation energies. Many theoretical investigations[13−21] have been devoted to determining the molecular structure of these compounds, but the dynamics of cis−trans isomerization in any of these compounds has still not been investigated.

We have performed classical trajectory calculations to analyze whether non-RRKM behavior, intrinsic and/or apparent, is exhibited in the cis−trans isomerization and F−O cleavage of nitrosyl hypofluorite (FONO). Our study begins with the construction of an analytical potential energy surface (PES) that models the above unimolecular processes in FONO, and goes on with the calculation of microcanonical rate constants $k(E)$ under two different types of initial sampling conditions: random distribution of vibrational energy and selective excitation of vibrational normal modes. Further work on the unimolecular dynamics of ClONO and BrONO is in progress.

Methods

A. Potential Energy Surface. We first constructed an analytical potential energy surface (PES) that describes the cis−

10.1021/jp982532w CCC: $15.00
Published on Web 10/10/1998

trans isomerization of FONO and the dissociation to F + ONO, based on data reported in the literature.[15,17,21−23] Our PES comprises anharmonic stretches, harmonic bends, and a torsional term represented by a truncated cosine series. Nondiagonal terms (such as sretch−stretch, stretch−bend, or bend−bend interactions) were not included in our PES because they produced spurious minima at large deviations from equilibrium, leading to significant errors in the dynamical calculations. Similar problems were reported by Guan and Thompson[8] in their investigation of the related molecule HONO. To model the system correctly at all regions of the PES, we have used switching functions that smoothly vary several parameters as the molecule dissociates or isomerizes. The form of the potential energy surface is

$$V = V(R_{FO}) + V(R_{O-N}) + V(R_{N=O}) + V(\theta_{FON}) + V(\theta_{ONO}) + V(\tau) \quad (2)$$

The F−O stretch is represented by the Morse function

$$V(R_{FO}) = D_{FO}\{1 - \exp[-\alpha_{FO}(R_{FO} - R_{FO,eq})]\}^2 \quad (3)$$

where D_{FO} is the potential well depth for the F−O stretching interaction, with different values for the cis (D_{FO}^{cis}) and trans (D_{FO}^{trans}) forms. α_{FO} is the curvature parameter, R_{FO} is the F−O distance, and $R_{FO,eq}$ is the equilibrium F−O bond distance parameter. The parameters α_{FO} and $R_{FO,eq}$ change according to the following expressions:

$$\alpha_{FO} = \alpha_{FO}^{cis} + (\alpha_{FO}^{trans} - \alpha_{FO}^{cis})SW1 \quad (4)$$

$$R_{FO,eq} = R_{FO}^{cis} + (R_{FO}^{trans} - R_{FO}^{cis})SW1 \quad (5)$$

where SW1 is a switching function given by

$$SW1 = 0.5\,(1 - \cos\tau) \quad (6)$$

with τ being the FONO torsional angle.

Similarly, the O−N and N═O stretches are represented by

$$V(R_i) = D_i\{1 - \exp[-\alpha_i(R_i - R_{i,eq})]\}^2 \quad (7)$$

where the subscript i makes reference to O−N or N═O. Different curvature and equilibrium bond length parameters were taken for FONO and ONO (a dissociation product). This forced us to introduce a switching function to vary these parameters gradually as the F−O bond dissociates:

$$\alpha_i = \alpha_i^p - (\alpha_i^p - \alpha_i^r)SW2 \quad (8)$$

$$R_{i,eq} = R_i^p - (R_i^p - R_i^r)SW2 \quad (9)$$

with

$$SW2 = \tanh^2\{Cl \exp[-C2(R_{FO} - R_{FO}^r)]\} \quad (10)$$

In eqs 8 and 9, the superscripts p and r refer to equilibrium values in ONO and FONO, respectively. In eq 10, the superscript r refers to cis or trans depending on the isomer from which the trajectories are initiated.

TABLE 1: Potential Energy Surface Parameters

Stretching Parameters

parameter	value/Å	parameter	value/Å^{-1}	parameter	value/(kcal/mol)
R_{FO}^{cis}	1.441[a]	α_{FO}^{cis}	4.00	D_{FO}^{cis}	16.53[b]
R_{FO}^{trans}	1.435[a]	α_{FO}^{trans}	4.32	D_{FO}^{trans}	14.07[b]
R_{O-N}^{r}	1.496[a]	α_{O-N}^{r}	1.26	D_{O-N}	40.7[d]
R_{O-N}^{P}	1.197[c]	α_{O-N}^{p}	4.05	$D_{N=O}$	114.8[d]
$R_{N=O}^{r}$	1.156[a]	$\alpha_{N=O}^{r}$	2.84		
$R_{N=O}^{p}$	1.197[c]	$\alpha_{N=O}^{P}$	2.41		

Bending Parameters

parameter	value/degrees	parameter	value/(aJ rad^2)
$\theta_{FON,eq}$	109.0[a]	K_{FON}	1.26
θ_{ONO}^{r}	115.0[a]	K_{ONO}	2.06
θ_{ONO}^{p}	134.0[c]		

Torsional Parameters

parameter	a_0	a_1	a_2
value/eV	0.2274	−0.0520	−0.2800

Switching Functions Parameters

parameter	C1	C2/Å^{-1}	C3/Å^{-2}	C4	C5/Å^{-2}	C6
value	6	6	1	2	1	2

[a] Taken from ref 15. [b] Taken from ref 21. [c] Taken from ref 23. [d] Taken from ref 7.

Quadratic functions attenuated by switching functions are employed to represent the FON and ONO bends:

$$V(\theta_{FON}) = 0.5K_{FON}(\theta_{FON} - \theta_{FON,eq})^2 SW2SW3 \quad (11)$$

$$V(\theta_{ONO}) = 0.5K_{ONO}(\theta_{ONO} - \theta_{ONO,eq})^2 SW3SW4 \quad (12)$$

where

$$SW3 = \exp(-C3(R_{O-N} - R_{O-N}^r)^{C4}) \quad (13)$$

$$SW4 = \exp(-C5(R_{N=O} - R_{N=O}^r)^{C6}) \quad (14)$$

The equilibrium bond angle $\theta_{ONO,eq}$ varies as the molecule dissociates:

$$\theta_{ONO,eq} = \theta_{ONO}^p - (\theta_{ONO}^p - \theta_{ONO}^r)SW2 \quad (15)$$

The superscripts r and p in eqs 13−15 refer to FONO and ONO, respectively.

The torsion interaction is modeled by a cosine series attenuated by the switching function SW2:

$$V(\tau) = \sum a_i \cos(i\tau)SW2 \quad (16)$$

where τ is the FONO dihedral angle.

Geometrical parameters (equilibrium bond lengths and equilibrium bond angles) for FONO were taken from ab initio data obtained by CCSD(T) calculations with a TZ2P basis set,[15] whereas for the product ONO we used experimental values.[22,23] The potential well depths for F−O (cis and trans) were taken from Lee et al.,[21] and those for O−N and N═O from Guan et al.[7] Most of the initial values for force constants and curvature parameters were taken from Lee and Rice,[15] but they were subsequently refined to reproduce more accurately the frequencies and energetics selected from the literature. Finally, the torsional coefficients a_i were obtained from a fit to CCSD(T)/TZ2P results.[17] All the parameters are listed in Table 1. A

TABLE 2: Normal Mode Frequencies (in cm^{-1}) for *cis*-Fono, *trans*-FONO, and ONO Radical

	cis-FONO		*trans*-FONO		ONO radical	
normal mode	PES	ab initio[a]	PES	ab initio[a]	PES	ab initio[b]
ω_1	233	271 (FON bend)	234	205 (torsion)	757	750
ω_2	332	355 (torsion)	305	305 (FON bend)	1255	1320
ω_3	520	399 (O−N stretch)	429	411 (O−N stretch)	1701	1634
ω_4	708	771 (ONO bend)	760	783 (ONO bend)		
ω_5	974	927 (F−O stretch)	984	954 (F−O stretch)		
ω_6	1741	1753 (N═O stretch)	1741	1758 (N═O stretch)		

[a] Taken from ref 15. Approximate descriptions of the normal vibrations are given in parentheses. [b] Taken from refs 22 and 23.

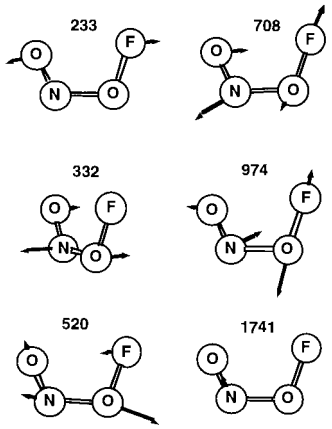

Figure 1. Depiction of the vibrational normal modes of equilibrium *cis*-FONO predicted by the PES developed in this study.

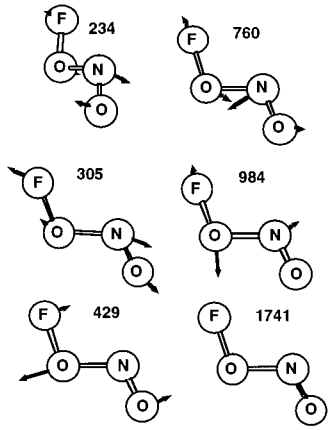

Figure 2. Depiction of the vibrational normal modes of equilibrium *trans*-FONO predicted by the PES developed in this study.

comparison of the frequencies calculated by our PES and those determined experimentally or by ab initio theory are shown in Table 2. Descriptions of the vibrational normal modes predicted by the analytical potential for the cis and trans isomers of FONO are depicted in Figures 1 and 2, respectively.

Our PES represents correctly the energetics of the cis−trans isomerization and F−O dissociation. The cis−trans energy difference is 2.4 kcal/mol, favoring the cis conformation, and the cis-to-trans barrier height is 14.1 kcal/mol. In addition, the F−O dissociation energies are predicted to be 16.5 and 14.1 kcal/mol for the cis and trans isomers, respectively. All these values coincide with the corresponding figures obtained by ab initio CCSD(T) calculations.[15,17,21]

B. Trajectory Calculations. We used the general classical trajectory code GenDyn[24] to perform the calculations. Hamilton's equations of motion were integrated in a lab-fixed Cartesian coordinate system by using a fourth-order Runge−Kutta-Gill routine with a fixed stepsize of 0.2 fs. The trajectories were calculated for 5 ps or until the isomerization or dissociation of the molecule took place. Energy conservation of at least three significant figures was achieved.

We employed ensembles of 1000 trajectories starting from either the cis or the trans conformation and two different methods to select the initial conditions. The first method was the "efficient microcanonical sampling" (EMS) procedure[25,26] as implemented in the GenDyn program. The sampling was carried out by performing a Markov walk in configuration space. We put into effect an initial Markov chain of 5×10^5 steps to ensure that the system was relaxed away from the initial configuration, and Markov chains of 10^4 moves between each individual trajectory. In each walk, the Cartesian coordinates of all four atoms were varied randomly up to a maximum displacement of 0.080 Å when we started from the cis isomer and 0.075 Å when we started from the trans isomer. These step sizes for the Markov walk led to approximately 50% acceptance of attempted moves.

Total energies in the range 19−45 kcal/mol (including the zero-point energies) were investigated with EMS initial conditions, when we started from the cis isomer. For trajectories initiated from the trans isomer, we explored the energy range 17−45 kcal/mol. Total angular momentum was restricted to zero.

The second method of initial conditions selection involved an initial distribution of zero-point energy in the six normal modes of vibration and then placing the rest of the energy up to a total energy of 30 kcal/mol into one of the normal modes of the molecule. A Monte Carlo phase averaging was used to obtain a random initial phase for each of the normal coordinates.

The rate constant for the global reaction $k_{\text{total}}(E)$ was obtained for each ensemble of trajectories by least-squares fitting of the lifetimes to the first-order equation

$$\ln(N_t/N_0) = -k_{\text{total}}(E)t \tag{17}$$

where N_t is the number of unreacted trajectories at time t and N_0 is the total number of trajectories in the ensemble (1000 trajectories). The rate constants for the two competing reactions, isomerization and dissociation, were obtained from

$$k_{\text{total}} = k_{\text{I}} + k_{\text{II}} \tag{18}$$

and

$$\frac{k_{\text{I}}}{k_{\text{II}}} = \frac{N_{\text{I}}}{N_{\text{II}}} \tag{19}$$

where k_{I} is the rate constant for the isomerization, k_{II} is the rate constant for the dissociation and N_{I} and N_{II} are the numbers of trajectories which led to isomerization and dissociation, respectively. The branching ratio $N_{\text{I}}/N_{\text{II}}$ was computed as a function of time.

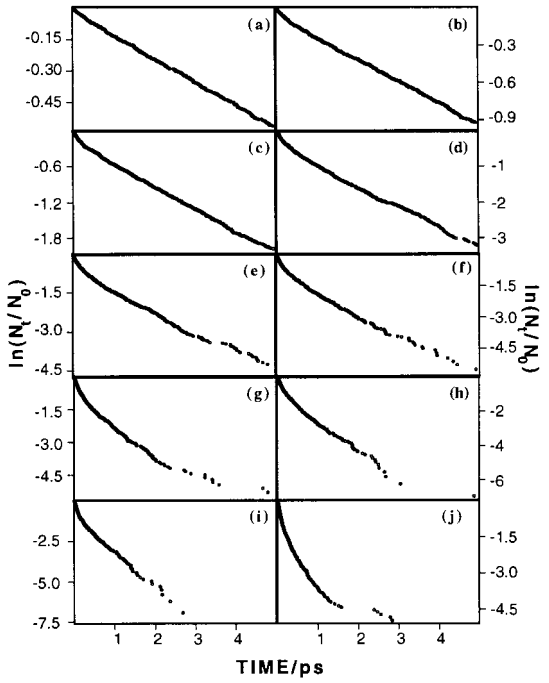

Figure 3. Decay curves computed for cis initialization at (a) 19.0 kcal/mol, (b) 20.0 kcal/mol, (c) 22.5 kcal/mol, (d) 25.0 kcal/mol, (e) 27.5 kcal/mol, (f) 30.0 kcal/mol, (g) 32.5 kcal/mol, (h) 35.0 kcal/mol, (i) 40.0 kcal/mol, and (j) 45.0 kcal/mol.

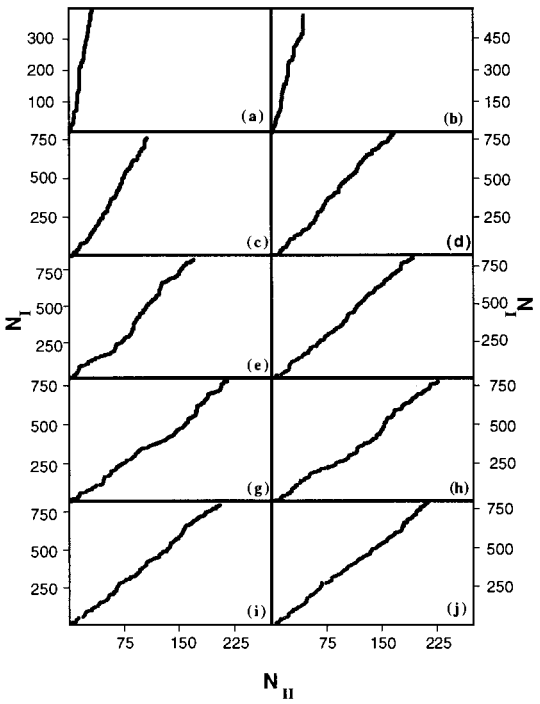

Figure 4. Branching ratios for cis initialization, displayed as a graph of $N_I(t)$ vs $N_{II}(t)$, obtained at (a) 19.0 kcal/mol, (b) 20.0 kcal/mol, (c) 22.5 kcal/mol, (d) 25.0 kcal/mol, (e) 27.5 kcal/mol, (f) 30.0 kcal/mol, (g) 32.5 kcal/mol, (h) 35.0 kcal/mol, (i) 40.0 kcal/mol, and (j) 45.0 kcal/mol.

Isomerization was assumed to have taken place when the system reached the top of the torsional barrier (93°),[17] but to check for immediate recrossing the trajectory was followed until the equilibrium angle of the other isomer was attained. The lifetime of the trajectory was taken as the time required to reach the top of the barrier. We considered that a trajectory led to dissociation if the F−O distance was longer than 3 Å. With this criterion, recrossings of trajectories were found to be negligible.

Results and Discussion

The rate constants for isomerization and dissociation were calculated over a wide range of energies with an initial microcanonical distribution of energy, starting from either the cis or the trans isomer. We have also evaluated the rate constants for initial conditions corresponding to excitation of each of the six normal modes at a total energy of 30 kcal/mol. All the calculations were performed with the angular momentum restricted to zero. This allowed us to make a direct comparison between the results obtained by the two different methods of initial sampling conditions described in the foregoing section. Additional calculations including angular momentum showed that rotational motion does not couple with vibrations. For the sake of simplicity, those results are not presented here.

The decay curves and the corresponding branching ratios computed under EMS initialization are shown in Figures 3−6. As can be seen, nonlinear behavior is enhanced as energy increases, suggesting intrinsic non-RRKM behavior. This nonlinearity indicates that the system evolves with a phase space bottleneck (or bottlenecks) so that transitions between different regions of phase space are less probable than the transition for crossing the transition state. As a result, the microcanonical ensemble is not maintained throughout the unimolecular dynamics.

The decay curves were fitted to the first-order expression given by eq 17 in order to obtain rough, time-averaged total

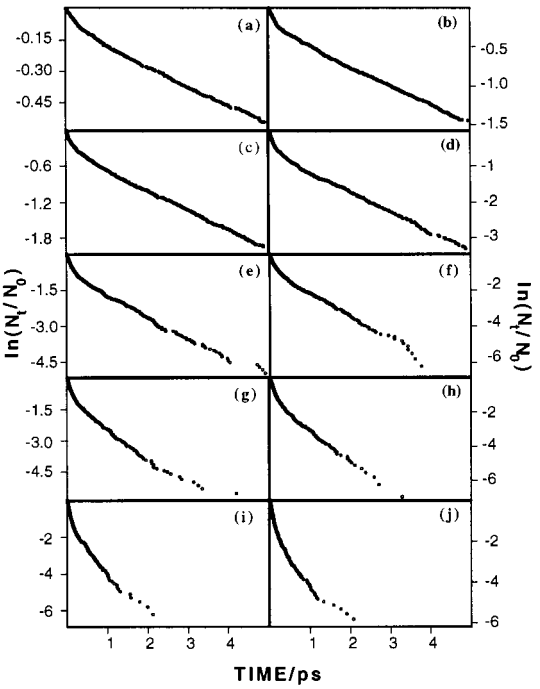

Figure 5. Decay curves computed for trans initialization at (a) 17.0 kcal/mol, (b) 19.0 kcal/mol, (c) 20.0 kcal/mol, (d), 22.5 kcal/mol, (e) 25.0 kcal/mol, (f) 27.5 kcal/mol, (g) 30.0 kcal/mol, (h) 35.0 kcal/mol, (i) 40.0 kcal/mol, and (j) 45.0 kcal/mol.

rate constants. Then the branching ratios estimated from Figures 4 and 6 were used to compute the individual rates. The total rate constants, the individual rate constants (isomerization and dissociation), and the branching ratios for cis initialization at total energies varying between 19 and 45 kcal/mol are shown in Table 3. The corresponding values for trans initialization are listed in Table 4. As can be seen, the isomerization rates

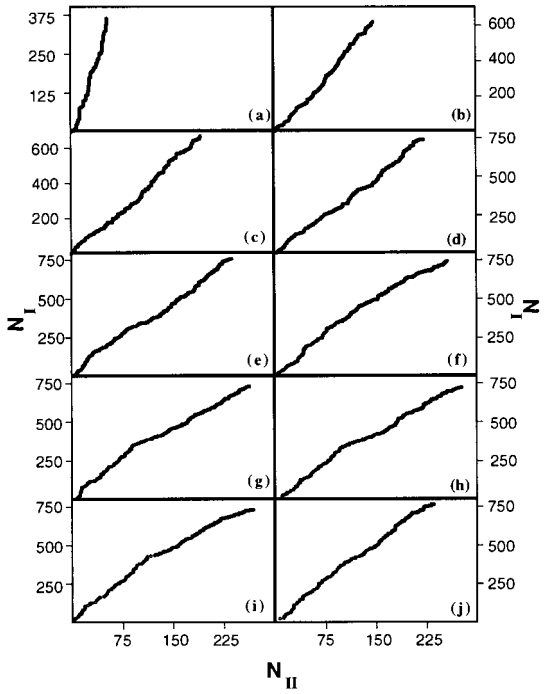

Figure 6. Branching ratios for trans initialization, displayed as a graph of $N_I(t)$ vs $N_{II}(t)$, obtained at (a) 17.0 kcal/mol, (b) 19.0 kcal/mol, (c) 20.0 kcal/mol, (d), 22.5 kcal/mol, (e) 25.0 kcal/mol, (f) 27.5 kcal/mol, (g) 30.0 kcal/mol, (h) 35.0 kcal/mol, (i) 40.0 kcal/mol, and (j) 45.0 kcal/mol.

TABLE 3: Decay Coefficients and Branching Ratios for cis Initialization

energy/(kcal/mol)	P[a]	k_{total}/ps^{-1}	k_I/ps^{-1}	k_{II}/ps^{-1}	N_I/N_{II}
19.0	42.9	0.111	0.103	0.008	13.58
20.0	60.3	0.180	0.166	0.014	12.22
22.5	86.3	0.400	0.351	0.049	7.17
25.0	96.1	0.66	0.54	0.11	4.90
27.5	98.7	0.97	0.81	0.17	4.87
30.0	99.7	1.33	1.07	0.26	4.21
32.5	99.6	1.67	1.30	0.37	3.47
35.0	100	2.14	1.66	0.49	3.39
40.0	100	2.90	2.32	0.58	3.97
45.0	99.4	2.93	2.30	0.64	3.61

[a] Percentages of reactive trajectories.

TABLE 4: Rate Coefficients and Branching Ratios for Trans Initialization

energy/(kcal/mol)	P[a]	k_{total}/ps^{-1}	k_I/ps^{-1}	k_{II}/ps^{-1}	N_I/N_{II}
17.0	41.9	0.105	0.091	0.0137	6.66
19.0	76.6	0.286	0.232	0.054	4.26
20.0	85.9	0.386	0.299	0.086	3.46
22.5	96.4	0.68	0.52	0.16	3.31
25.0	99.4	1.14	0.87	0.28	3.16
27.5	99.9	1.63	1.23	0.40	3.07
30.0	99.7	1.89	1.40	0.49	2.85
35.0	100	2.65	1.94	0.71	2.72
40.0	99.9	3.95	2.95	0.99	2.98
45.0	99.8	4.28	3.31	0.97	3.40

[a] Percentages of reactive trajectories.

are substantially higher than the dissociation rates, and the branching ratios N_I/N_{II} decrease with increasing energy, from 13.58 to 3.61 for cis initialization and from 6.66 to 3.40 for trans initialization. These results could be expected because the F−O dissociation energies are higher than the isomerization barriers. On the other hand, the rate constants for cis initialization are significantly smaller than those for trans initialization. This could be expected as well because both the F−O

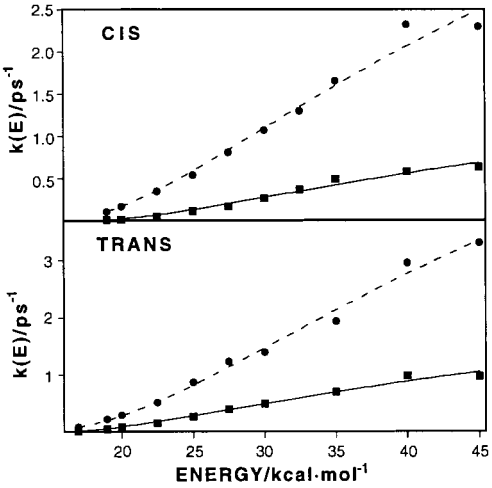

Figure 7. Isomerization (circles) and dissociation (squares) rate constants as a function of the total energy for cis and trans initializations under EMS conditions. The lines are the fits to the RRK expression (eq 20).

dissociation energy and the isomerization barrier for *cis*-FONO are higher than the corresponding quantities for *trans*-FONO.

We have fitted the individual rate constants to the RRK expression[1,2]

$$k(E) = \nu\left(\frac{E - E_0}{E}\right)^{(s-1)} \qquad (20)$$

where E_0 is the barrier height for the isomerization or the dissociation, s is the number of degrees of freedom among which the total energy E is assumed to be randomized, and ν is a frequency factor. Figure 7 shows the fits corresponding to cis and trans initializations. For cis initialization, the s values attained from the fits are 4.2 (isomerization) and 3.6 (dissociation); for trans initialization, the values are 5.2 (isomerization) and 3.9 (dissociation). In general, these values are somewhat low compared to the total number of vibrational modes. Qualitatively, this suggests that some of the modes are not substantially coupled to the reaction coordinates, which corroborates our previous results indicating intrinsic non-RRKM behavior. Fits of the classical RRK expression (eq 20) to trajectory results frequently afford values for s that are significantly smaller than the "theoretical" values $3N-6$.[27] We should note that the RRK expression involves the harmonic approximation, which is appropriate for experimental conditions since the average energy per mode is often low. However, this approximation fails when the energy is relatively high, which is often the case of trajectory calculations. Therefore, deviations between RRK theory and our trajectory results might to some extent be arisen from the anharmonic nature of the stretching interactions in our model PES.

We have also evaluated the rates of isomerization and dissociation resulting from initial excitation of each normal mode. The decay curves and branching ratios obtained for an initial total energy of 30 kcal/mol are shown in Figures 8 and 9. The plots, arranged in order of increasing wavenumber of the excited mode, are very different depending on the mode initially excited. Although in most cases the decay curves are nearly linear, some of them, e.g., plots 8g, 8c′, or 8g′ show a small time delay (less than 1 ps) before any isomerizations or dissociations occur. This indicates that energy transfer to the reaction coordinate is slow when these normal modes are excited. On the contrary, plots 8c and 8b′, which correspond

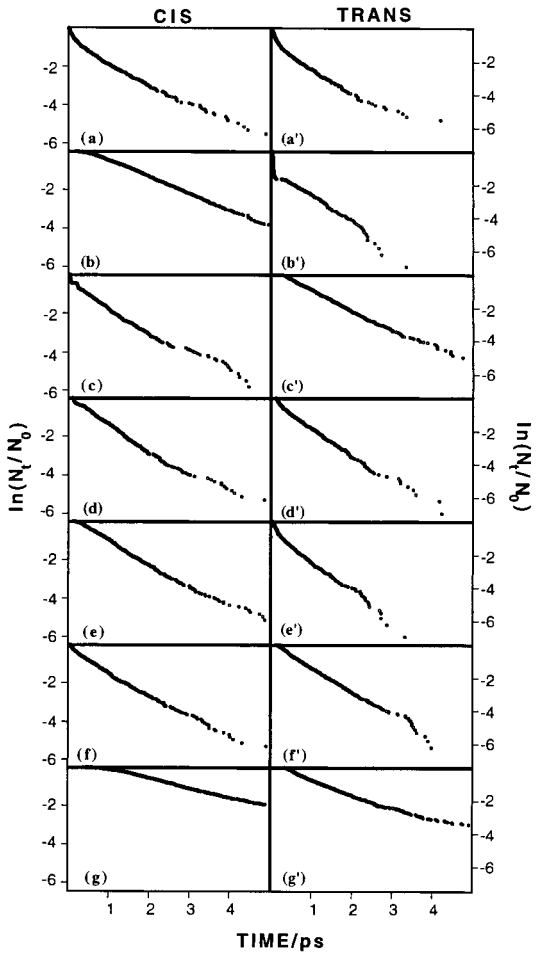

Figure 8. Decay curves computed at a total energy of 30 kcal/mol for cis initialization under (a) EMS conditions, (b) mode-excited 233, (c) mode-excited 332, (d) mode-excited 520, (e) mode-excited 708, (f) mode-excited 974, (g) mode-excited 1741, and for trans initialization under (a′) EMS conditions, (b′) mode-excited 234, (c′) mode-excited 305, (d′) mode-excited 429, (e′) mode-excited 760, (f ′) mode-excited 984, and (g′) mode-excited 1741.

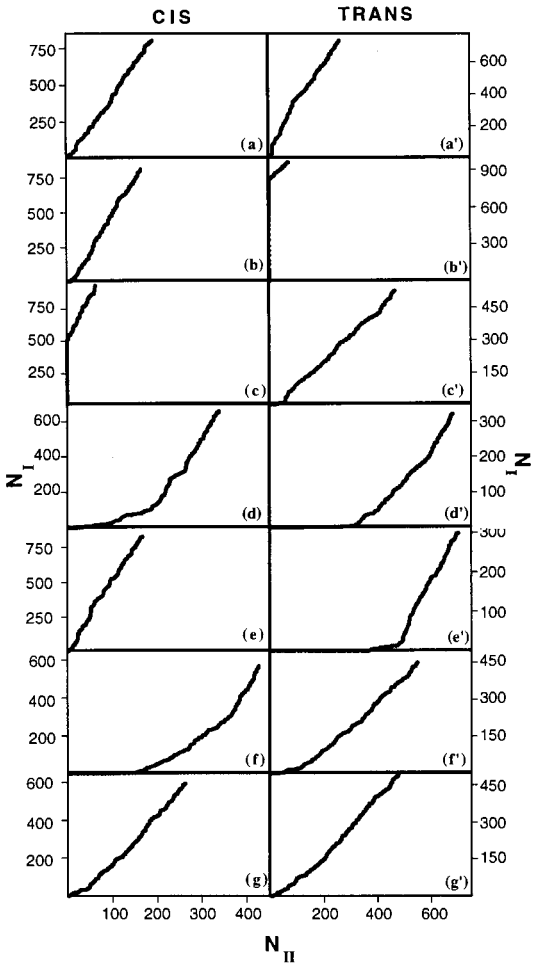

Figure 9. Branching ratios for cis initialization under (a) EMS conditions, (b) mode-excited 233, (c) mode-excited 332, (d) mode-excited 520, (e) mode-excited 708, (f) mode-excited 974, (g) mode-excited 1741, and for trans initialization under (a′) EMS conditions, (b′) mode-excited 234, (c′) mode-excited 305, (d′) mode-excited 429, (e′) mode-excited 760, (f ′) mode-excited 984, and (g′) mode-excited 1741.

to initial excitation of mode 332 in the cis isomer and mode 234 in the trans isomer, respectively, present an initial rapid decay. This is due to the fact that the excited mode is the isomerization coordinate (FONO torsion), leading to almost immediate isomerization before energy randomization is reached. The associated branching ratios, plots 9c and 9b′, corroborate the previous explanation: the curves show that a great number of isomerizations took place before the first dissociations occurred. There are several more plots in which one of the two reactions, isomerization or dissociation, is dramatically favored during the initial stages. The nonlinearity observed in most of the branching rations as well as the time delay observed in several decay curves are evidences for nonstatistical behavior. As these facts are found under nonrandom excitation, it can be concluded that the system exhibits apparent non-RRKM behavior.[3,4]

Total and individual rate constants estimated under initial excitation of each normal mode are given in Tables 5 and 6. We remark that it was not our intention here to calculate accurate rate constants; rather, our aim was to explore the isomerization and dissociation dynamics of FONO from a qualitative point of view in order to get insight into the statistical versus nonstatistical behavior of these processes. For cis initialization, there is no total rate constant that is significantly higher than that computed under statistical conditions (1.33 ps^{-1}), standing

TABLE 5: Rate Coefficients and Branching Ratios for Cis Initialization Resulting from Excitation of Each Normal Mode (Indicated by Its Wavenumber)

ensemble	k_{total}/ps^{-1}	k_I/ps^{-1}	k_{II}/ps^{-1}	N_I/N_{II}
EMS	1.33	1.07	0.26	4.21
233	0.84	0.70	0.14	5.06
332	1.36	1.28	0.086	14.93
520	1.36	0.84	0.52	1.62
708	1.23	1.02	0.20	5.07
974	1.26	0.64	0.62	1.04
1741	0.50	0.34	0.15	2.27

TABLE 6: Rate Coefficients and Branching Ratios for Trans Initialization Resulting from Excitation of Each Normal Mode (Indicated by Its Wavenumber)

ensemble	k_{total}/ps^{-1}	k_I/ps^{-1}	k_{II}/ps^{-1}	N_I/N_{II}
EMS	1.89	1.40	0.49	2.85
234	2.01	1.94	0.068	28.46
305	1.21	0.63	0.58	1.10
429	1.75	0.46	1.28	0.36
760	2.13	0.50	1.63	0.30
984	1.50	0.66	0.84	0.78
1741	0.89	0.45	0.44	1.02

out the low values corresponding to excitation of modes 233 (0.84 ps^{-1}) and 1741, the N═O stretch (0.50 ps^{-1}). Excitation of the N═O stretching mode in HONO[7,8] also resulted in a slow

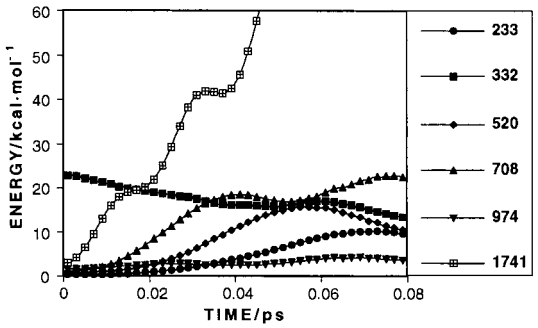

Figure 10. Normal-mode energy versus time averaged over 1000 trajectories for selective excitation of mode 332 in the cis isomer. The legend indicates the normal mode by its wavenumber.

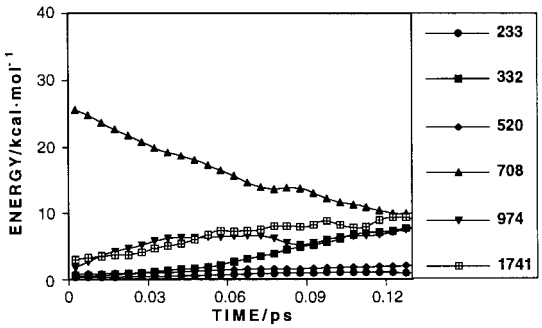

Figure 11. Normal-mode energy versus time averaged over 1000 trajectories for selective excitation of mode 708 in the cis isomer. The legend indicates the normal mode by its wavenumber.

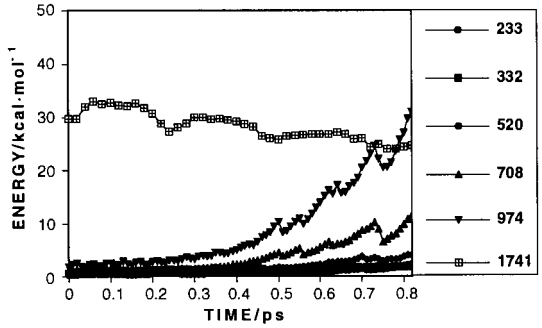

Figure 12. Normal-mode energy versus time averaged over 1000 trajectories for selective excitation of mode 1741 in the cis isomer. The legend indicates the normal mode by its wavenumber.

rate. The differences in the computed values increase when we compare the individual rate constants. Thus, the isomerization rate constants range from 0.34 ps^{-1} (excitation of mode 1741) to 1.28 ps^{-1} (excitation of mode 332, the reaction coordinate for cis→trans isomerization), and the dissociation rate constants range from 0.086 ps^{-1} (mode 332) to 0.62 (mode 974: closely related to the dissociation coordinate).

The rates computed for trans initialization show even more disparity than found for cis initialization. Note that the branching ratios are in general smaller than those predicted for cis initialization, although excitation of mode 234 (the torsional mode for *trans*-FONO) led to the largest value (28.46). In particular, initial excitations of modes 429, 760, and 984, for which the eigenvectors of the normal modes of vibration indicate a significant contribution from the F−O stretch (see Figure 2), resulted in branching ratios smaller than unity, that is, dissociation is faster than isomerization.

Couplings between vibrational modes can be explored from a qualitative point of view by monitoring the normal-mode energies for the first picoseconds. This type of analysis can reveal whether there is a preferred pathway for energy transfer. For the sake of example, we have selected the ensembles of trajectories corresponding to initial excitations of modes 332, 708, and 1741, all of them concerning cis initialization. Excitation of mode 332 led to a total rate constant (1.36 ps^{-1}) similar to that computed under statistical initial conditions (1.33 ps^{-1}). The calculated value for the isomerization rate constant, 1.28 ps^{-1}, is larger than the statistical result, 1.07 ps^{-1}. This seems somewhat striking because mode 332 is the torsional mode in the cis isomer, that is, the reaction coordinate for cis→trans isomerization, and so a much greater enhancement of the isomerization rate constant would be expected. To investigate this in more detail, the normal mode energies for the first 0.08 ps were monitored for an ensemble of 1000 trajectories under initial excitation of normal mode 332 at a total energy of 30 kcal/mol. The results are shown graphically in Figure 10. As can be seen, energy rapidly transfers out of this mode into many other modes, specially into mode 1741 (N═O stretch), which is characterized by the lowest rate constant. This clarifies why the isomerization rate constant is not dramatically enhanced with respect to the statistical value. Furthermore, mode 974, which presents a substantial contribution from the F−O stretch (associated to the dissociation coordinate), do not receive appreciable energy during the period of time studied. This accounts for the very small value predicted for the dissociation rate.

From a simple inspection of the normal mode eigenvectors (see Figure 1), one could expect that excitation of mode 708 in the cis isomer would enhance the dissociation rate. However, the estimated branching ratio is 5.07, slightly higher than that computed for the microcanonical ensemble. Figure 11 shows the redistribution of vibrational energy when mode 708 is initially excited. As can be seen, energy is quickly transferred into modes 332, 974, and 1741, but not into mode 520, which shows together with mode 974 enhancement of the dissociation rate. This explains why the dissociation channel is not significantly favored in mode-excited 708 with respect to the statistical case.

Figure 12 shows the averaged normal mode energies for trajectories from mode-excited 1741 for which the lowest rate was predicted. In this case we followed the energy transfer up to a much longer time, 0.85 ps. Energy seems to be trapped in this mode (N═O stretch), similarly to that found for MeONO,[11] and only after 0.4 ps energy is transferred into modes 974 and 708, the former showing enhancement of the dissociation rate constant. Mode 1741 is thus a bottleneck for IVR and this confirms our previous suggestion that the system presents intrinsic non-RRKM behavior. These observations clarify the low values of the rate constants computed under initial excitation of mode 1741 and why the branching ratio N_I/N_{II} diminishes significantly with respect to the EMS value.

The problem that classical mechanics does not conserve quantum zero-point energy (ZPE) in vibrational modes is well-known.[28] It seems interesting to analyze whether the ZPE does not tend to preferentially leak out of the normal modes during the time scale for reaction. To this end, we present in Figure 13 plots of the energy in the normal modes as a function of time for the cis and trans isomers with initial energy corresponding to the ZPE. The total zero-point energies for the cis and trans isomers are 6.45 and 6.37 kcal/mol, respectively. As can be seen, the ZPE in each mode is basically maintained throughout the period of time considered (1 ps), suggesting that, for the system studied here, the ZPE problem of classical trajectories should not be significant.

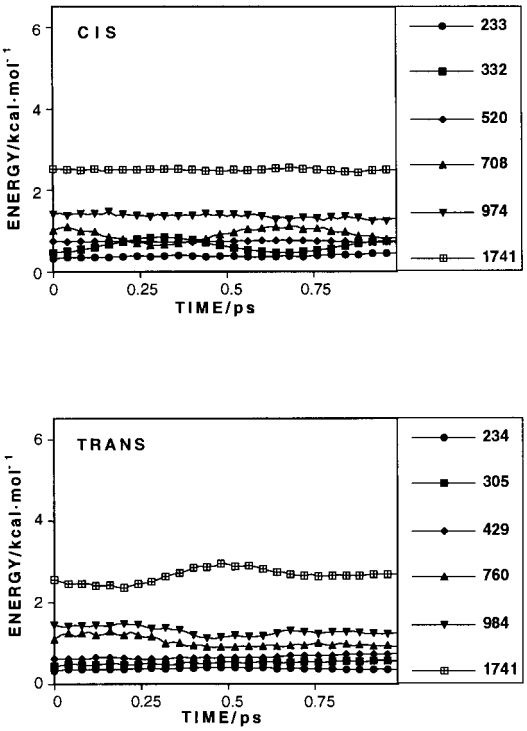

Figure 13. Normal-mode energy versus time averaged over 1000 trajectories for the cis and trans isomers with initial energy corresponding to the ZPE.

Concluding Remarks

Classical trajectory calculations were performed to explore whether nonstatistical behavior is present in the cis−trans isomerization and F−O dissociation of nitrosyl hypofluorite. For this purpose, a potential energy function that describes the above unimolecular processes was constructed on the basis of ab initio and experimental data.

The decay curves obtained at energies in the range 17−45 kcal/mol and employing statistical initial conditions are in most cases nonlinear, suggesting intrinsic non-RRKM behavior. Least-squares fits of our trajectory results to the RRK expression, eq 20, led to *s* values significantly smaller than the theoretical value 3*N*-6, which is in line with the above suggestion.

Under EMS conditions, the isomerization rates are much larger than the F−O bond fission rates, although the branching ratios decrease with increasing energy. In addition, we found that the rates obtained for cis initialization are smaller than the corresponding rates calculated for trans initialization. These results are as expected on account of the energetics of these unimolecular processes.

The calculations performed under selective excitation of vibrational modes at a total energy of 30 kcal/mol indicates that the rates of isomerization and F−O dissociation are strongly dependent on the mode in which energy is initially deposited, that is, apparent non-RRKM behavior is also exhibited in the unimolecular processes investigated here. We found that the F−O bond fission is favored over the isomerization process when any of the modes 429, 760, or 984 in the trans isomer is initially excited.

Acknowledgment. A.P.-G. and E.M.-N. thank Fundación Gil Dávila and Xunta de Galicia, respectively, for their grants.

References and Notes

(1) Holbrook, K. A.; Pilling, M. J.; Roberston, S. H. *Unimolecular Reactions*, 2nd ed.; John Wiley & Sons: Chichester, 1996.

(2) Bunker, D. L. *Theory of Elementary Gas Reaction Rates*, Pergamon: London, 1966.

(3) Bunker, D. L.; Hase, W. L. *J. Chem. Phys.* **1973**, *59*, 4621.

(4) Baer, T.; Hase, W. L. *Unimolecular Reaction Dynamics, Theory and Experiments*; Oxford University Press: New York; Chapter 8.

(5) McDonald, P. A.; Shirk, J. S. *J. Chem. Phys*. **1982**, *77*, 2355.

(6) Shirk, A. E.; Shirk, J. S. *Chem. Phys. Lett.*, **1983**, *97*, 549.

(7) Guan, Y.; Lynch, G. C.; Thompson, D. L. *J. Chem. Phys*. **1987**, *87*, 6957.

(8) Guan, Y.; Thompson, D. L. *Chem. Phys*. **1989**, *139*, 147.

(9) Preiskorn, A.; Thompson, D. L. *J. Chem. Phys*. **1989**, *91*, 2299.

(10) Qin, Y.; Thompson, D. L. *J. Chem. Phys*. **1992**, *96*, 1992.

(11) Martínez-Núñez, E.; Vázquez, S. A. *J. Chem. Phys*. **1997**, *107*, 5393.

(12) DeMore, W. B.; Sander, S. P.; Golden, D. M.; Hampson, R. F.; Kurylo, M. J.; Howard, C. J.; Ravishankara, A. R.; Kolb, C. E.; Molina, M. J. Chemical Kinetics and Photochemical Data for Use in Stratospheric Modeling. Evaluation No. 10, August 15, 1992; NASA JPL Publication 92-20; National Aeronautics and Spa. Administration: Washington, DC, 1992.

(13) Vance, R.; Turner, A. G. *Inorg. Chim. Acta* **1988**, *149*, 95.

(14) Dixon, D. A.; Christe, K. O. *J. Phys. Chem*. **1992**, *96*, 1018.

(15) Lee, T. J.; Rice, J. E. *J. Chem. Phys*. **1992**, *97*, 4223.

(16) Amos, R. D.; Murray, C. W.; Handy, N. C. *Chem. Phys. Lett*. **1993**, *202*, 489.

(17) Cárdenas-Jirón, G. I.; Toro-Labbé, A. *Chem. Phys. Lett*. **1994**, *222*, 8.

(18) Lee, T. J.; Bauschlicher, C. W., Jr.; Dateo, C. D.; Rice, J. E. *Chem. Phys. Lett*. **1994**, *228*, 583.

(19) Lee, T. J. *J. Phys. Chem*. **1994**, *98*, 111.

(20) Lee, T. J. *J. Phys. Chem*. **1996**, *100*, 19847.

(21) Lee, T. J.; Rice, J. E.; Dateo, C. E. *Mol. Phys*. **1996**, *89*, 1359.

(22) Ervin, K. M.; Ho, J.; Lineberger, W. C. *J. Phys. Chem*. **1988**, *92*, 5405.

(23) Yu, D.; Rauk, A.; Armstrong, D. A. *J. Phys. Chem*. **1992**, *96*, 6031.

(24) We are very grateful to Dr. D. L. Thompson co-workers for their generous provision of the GenDyn program.

(25) Nyman, G.; Nordholm, S.; Schranz, H. W. *J. Chem. Phys*. **1990**, *93*, 6767.

(26) Schranz, H. W.; Nordholm, S.; Nyman, G. *J. Chem. Phys*. **1991**, *94*, 1487.

(27) Shalashilin, D. V.; Thompson, D. L. *J. Chem. Phys*. **1996**, *105*, 1833.

(28) McCormack, D. A.; Lim, K. F. *J. Chem. Phys*. **1997**, *106*, 572 and references therein.